Numerical investigation of multiple slot jets in air knife coating

A. Yahyaee Soufiani[1], J.R. McDermid[2], A.N. Hrymak[3] and F.E. Goodwin[4]

[1]McMaster University
1280 Main street west, Hamilton, ON, Canada, L8S 4L8
Phone: (289) 527-4435
Email: yahyaea@mcmaster.ca

[2]McMaster University
1280 Main Street West, Hamilton, ON, Canada, L8S 4L8
Phone: (905) 525-9140 Ext 27476
Email: mcdermid@mcmaster.ca

[3]University of Western Ontario
1151 Richmond St N, London, ON, Canada, N6A 5B9
Phone: (519) 661-2128
Email: ahrymak@uwo.ca

[4]International Zinc Association
2530 Meridian Parkway, suite 115, Durham, NC, USA 27713
Phone: (919) 287-1878
Email: fgoodwin@zinc.org

1. Introduction

Hot dip galvanizing is a coating technique which is commonly used in the steel industry. The molten zinc coating thickness of on the sheet substrate is usually controlled through the use of a planar gas jet or air knife, typically in a single slot configuration. The film thickness can be reduced by applying a turbulent air jet, which impinges on the coated substrate just above the bath surface to wipe the excess fluid from the substrate. Because of the pressure gradient and shear stress applied to the liquid film by the jet, only a small portion of the film can be carried by the moving substrate, where the majority of the liquid returns to the bath as a runback flow [1-4]. The film thickness after wiping, h_f , depends on the substrate velocity V_s, the nozzle pressure P_0 , the nozzle to substrate standoff distance *z*, the nozzle slot width, *d*, as well as the liquid properties. [5-6].

Thornton and Graff [1] proposed a model for calculating the final film thickness by assuming that the reduction of film thickness was due solely to the pressure gradient created by the impinging jet. Tuck [2] used a similar approach and checked the stability of the solutions for long wavelength perturbations. Ellen and Tu [3] presented a model which took the shear stress into account, as well as the pressure gradient, when calculating the final liquid coating thickness.

The objective of this paper is to investigate the effect of multiple-slot air jets on the final coating thickness through numerical simulations to determine if there are operating regions that are most robust to air knife profile changes. The schematic figure of the two nozzle geometries is illustrated in Figure 1. This study emphasizes the effects of pressure gradient and shear stress distribution induced by the multiple jets on the estimate of the final coating thickness.

For the numerical simulations, dimensions of the auxiliary jet width (*a*), distance between the exit of the main and auxiliary jet (*s*), and the main jet slot width (*d*) are 3 mm, 19.7 mm and 1.5 mm respectively. The inclination of the auxiliary jets from the main jet is 20^o. The mesh used for the impinging jets was comprised of a mixture of quadrilaterals and triangles. The full physical domain was solved, not taking into account geometrical symmetry.

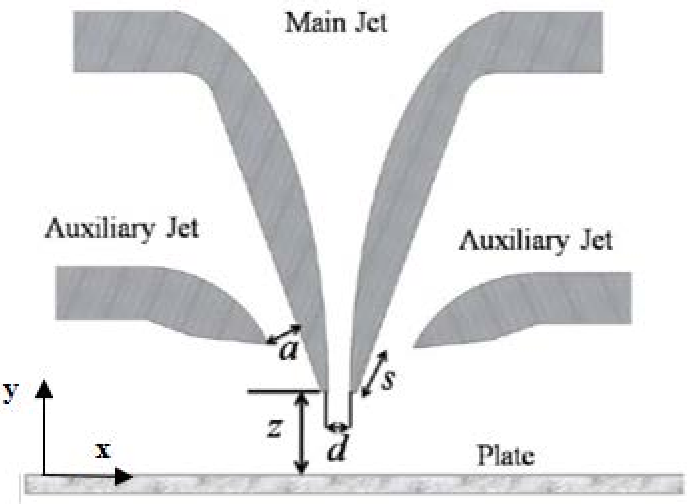

Figure 1) Schematic of multiple slot jets

Grid clustering was used close to the wall and around the centerline where there are large gradients. Four grids, with increasing numbers of nodal points, were tested to ensure mesh independence of the numerical results.

In order to determine the operating window, different geometrical parameter values for the multiple slot jets were considered in the numerical simulations and the results compared. Moreover, a parametric study, including the main and auxiliary jet Reynolds numbers, jet to wall distance and velocity of the substrate was performed and the effect on final film thickness determined.

2. Mathematical Formulation

Calculation of volumetric flux of the liquid zinc on the steel strip, q, is the first step in the modeling of the coating thickness [8]. A condensed summary of the analysis is provided below. A simplified form of the Navier-Stokes equation can be used for calculating q based on the assumptions of steady-state, isothermal, incompressible flow of the liquid film, where it is assumed that surface tension can be neglected and that the no-slip condition of the liquid on the steel strip is valid [7-9]. Fluid properties, such as viscosity and density, were assumed to be constant. By considering the above assumptions, the two-dimensional Navier-Stokes equation for a thin film on a flat plate reduces to:

$$\mu \frac{d^2u}{dy^2} - (\rho g + \frac{dp}{dx}) = 0 \tag{1}$$

The boundary conditions are given by:

$$u = V_s \qquad \text{at } y=0 \tag{2}$$

$$\mu\left(\frac{\partial u}{\partial y}\right) = \tau \qquad \text{at } y = w \tag{3}$$

Where, w is local film thickness.

Integrating equation (1) and applying the boundary conditions (2) and (3) yields:

$$u = V_s\left[1+\frac{y}{w}SW-\frac{y}{w}\left(2-\frac{y}{w}\right)\frac{GW}{2}\right] \tag{4}$$

Where $W = w\sqrt{\frac{\rho g}{\mu V_S}}$ is the non-dimensional film thickness, $S = \frac{\tau}{\sqrt{\rho\mu V_S g}}$ is the non-dimensional shear stress; and $G = 1+\frac{1}{\rho g}\frac{dp}{dx}$ is the effective gravitational acceleration.

The volumetric flux of the liquid, q, can then be calculated as:

$$q = \int_0^w u dy = V_s w\left(1+\frac{SW}{2}-\frac{GW^2}{3}\right) \tag{5}$$

The withdrawal flux, $Q = \frac{q}{V_S}\sqrt{\frac{\rho g}{\mu V_S}}$ be derived from equation (5) by substitution and rearrangement as:

$$Q = -\frac{GW^3}{3}+\frac{SW^2}{2}+W \tag{6}$$

From Elsaadawy et al. [8], the non-dimensional film thickness W, corresponding to the maximum withdrawal flux, $Q_{\max}$, can be determined by solving $\frac{dQ}{dW}=0$ and employing the quadratic formula such that:

$$W = \frac{S \pm \sqrt{S^2+4G}}{2G} \tag{7}$$

Using the above formalism, the non-dimensional film thickness is a function of dp/dx, τ at any coordinate x. Due to mass continuity, the minimum value of $Q_{\max}$ corresponding to every x value is the physically available withdrawal flux, Q [8]. The final coating thickness, h_f is given by

$$h_f = \frac{q}{V_S} = \frac{(Q_{\max})_{\min}}{\sqrt{\frac{\rho g}{\mu V_S}}} \tag{8}$$

The distribution of shear stress and pressure gradient along the wall can be used in the equations (7) and (8) to estimate the final coating thickness on a moving substrate.

3. Discussion

A computational fluid dynamics (CFD) approach was used to model the steady-state pressure distribution and shear stress on the wall using ANSYS FLUENT 14.0. The SIMPLE method was used for pressure-velocity coupling. The standard method, where pressure values are interpolated using the cell face center values, was used for the pressure term. The second order upwind scheme was used for the momentum, turbulent kinetic energy and turbulent dissipation rate. The turbulent kinetic energy – dissipation rate (k-ε) method was used for the turbulence model.

3.1. Validation

Numerical simulations versus experimental data on wall pressure distribution and pressure gradient for $4 \leq z/d \leq 12$ at Re_m=11000 are presented in this section. Figure 2a presents a comparison of numerical non-dimensional wall pressure profile versus the experimental data of Ritcey [9] for a short nozzle single-slot planar impinging jet as function of z/d. It can be seen that the value of the predicted maximum non-dimensional pressure and the pressure distribution were in good agreements with the experimental data. Figure 2b shows the numerically derived pressure gradient versus the experimental pressure gradient for $4 \leq z/d \leq 12$ at Re_m=11000. It can also be seen from Figure 2b that the simulated maximum pressure gradient matches very well with the corresponding experimental measurements. Figure 3 compares the numerical and experimental results for the wall skin friction, $C_f = \tau_w / (0.5 \rho U^2)$. The numerical skin friction results are lined up very well with the corresponding experimental measurements of Ritcey [9]. It can be seen that the maximum C_f value decreased with increasing *z/d*. The decreasing skin friction can be attributed to the decaying velocity of the jet and momentum loss due to fluid entrainment.

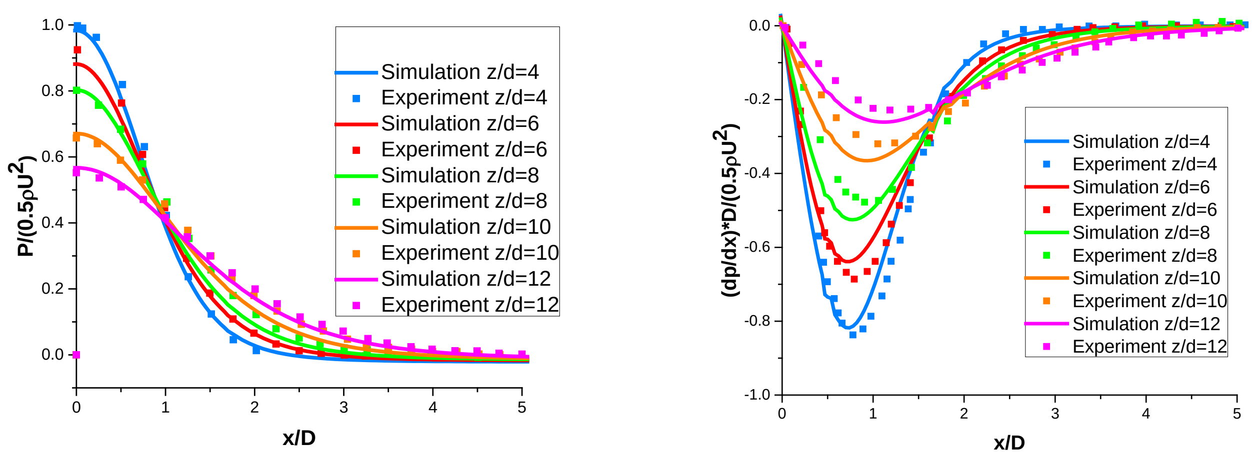

Figure 2) Comparison of a) pressure distribution and b) pressure gradient predicted by numerical simulation versus the experimental measurements of Ritcey [9] for a single slot jet.

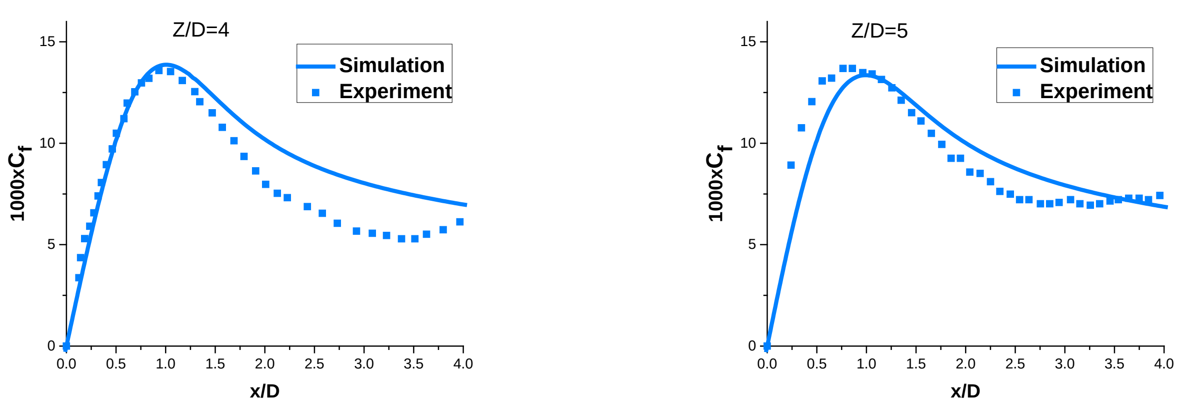

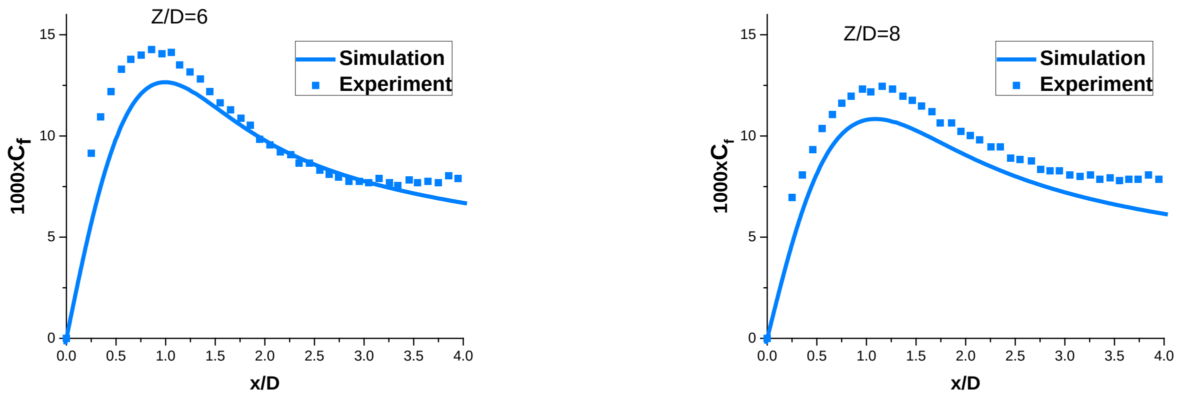

Figure 3) Comparison of numerical and experimental wall shear stress profiles for a) z/d=4, b) z/d=5, c) z/d=6, d) z/d=8

3.2. Effect of jet to wall distance (z/d)

By increasing the jet to wall distance, *z/d*, both the maximum shear stress and maximum pressure gradient decreased and consequently an increase in final coating thickness was observed (Figure 4). By comparing single jet and multiple jets, it was found that at each specific *z/d* the maximum shear stress and maximum pressure gradient were lower versus the single slot design, so consequently the coating weight was higher than that of the single jet (Figure 5a-5b).

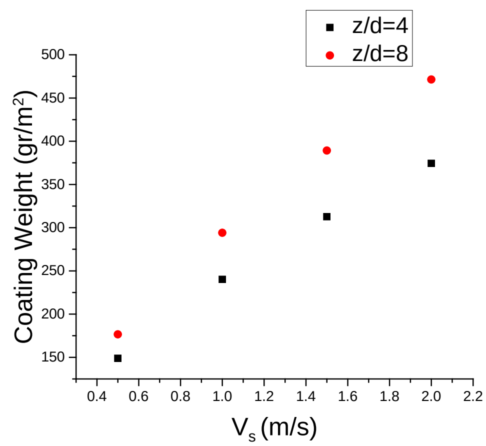

Figure 4) Coating weight results as a function of strip velocity for multiple slot jets, Re_m=11000, Re_a=11000

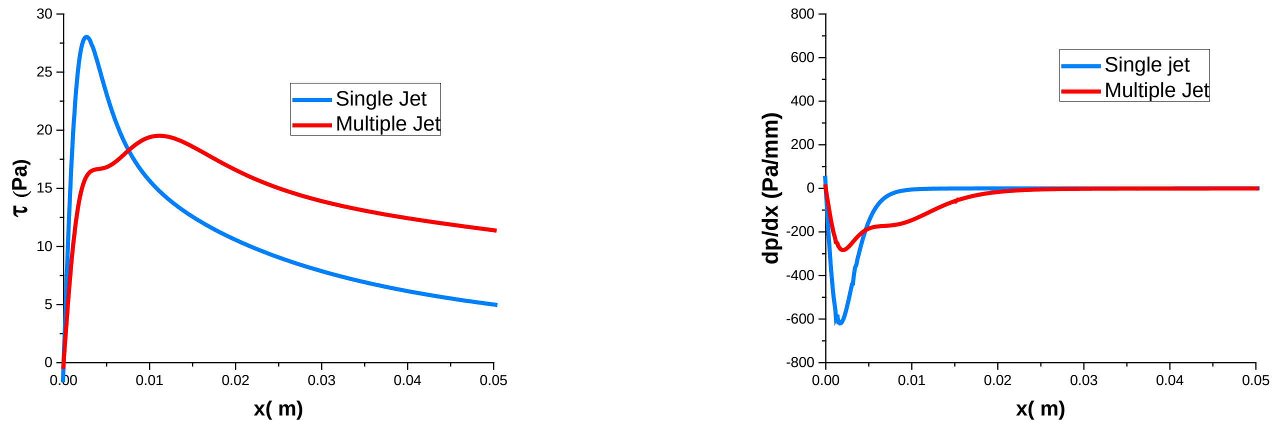

a b

Figure 5) Comparison a) wall shear stress b) wall pressure gradient of single and multiple jet results for Re_m=11000, Re_a=11000, z/d=6

By superimposing streamlines on the pressure contour (Figure 6) it can be seen that entrainment of auxiliary jet flow into the main jet flow the flow makes the pressure profile wider. This would explain why both the maximum pressure gradient and maximum shear stress for multiple jet was lower than single jet case.

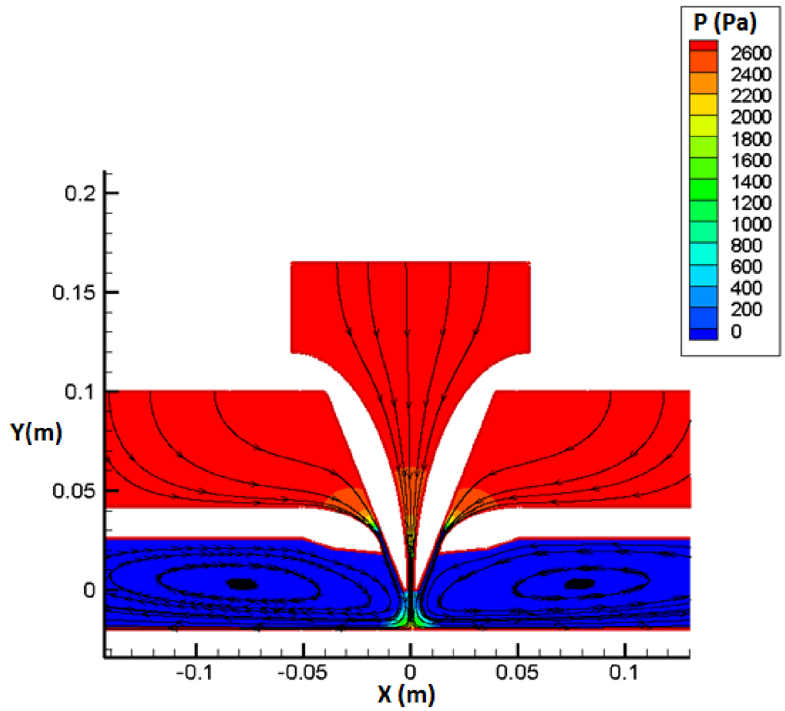

Figure 6) Streamline and pressure contour of Multiple slot jets, Re_m=11000, Re_a=11000, z/d=6

3.3. Effect of strip velocity on coating weight

Figure 7 shows the variation of coating weight as a function of strip velocities ranging from 0.5 to 2.50 *m/s* for z/d=8 with Re_m=11000 and Re_a=11000 for the multiple jet case. By increasing the strip velocity the coating weight increased continuously, as would be expected.

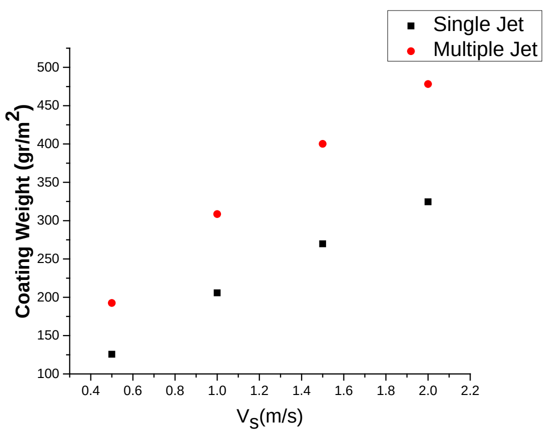

Figure 7) Effect of strip velocity on coating weight for Re_m=11000, $Re_{a=}$11000, z/d=6

3.4. Effect of Auxiliary Jet Reynolds Number (Re_a)

Figure 8 shows wall pressure gradient and shear stress profile for Re_a of 7500 and 15000 for a fixed Re_m=11000 and z/d=8. It can be seen from Figure 7 that in the wall region, higher jet momentum can be achieved due to presence of the auxiliary jets and the maximum shear stress shifted downstream as a result of increasing the auxiliary jet Reynolds number. However, since both the maximum shear stress and maximum pressure gradient are significantly lower than for the single jet, the final coating weight would increase with increasing auxiliary jet Re for the multiple jet desgin. (Figure 9)

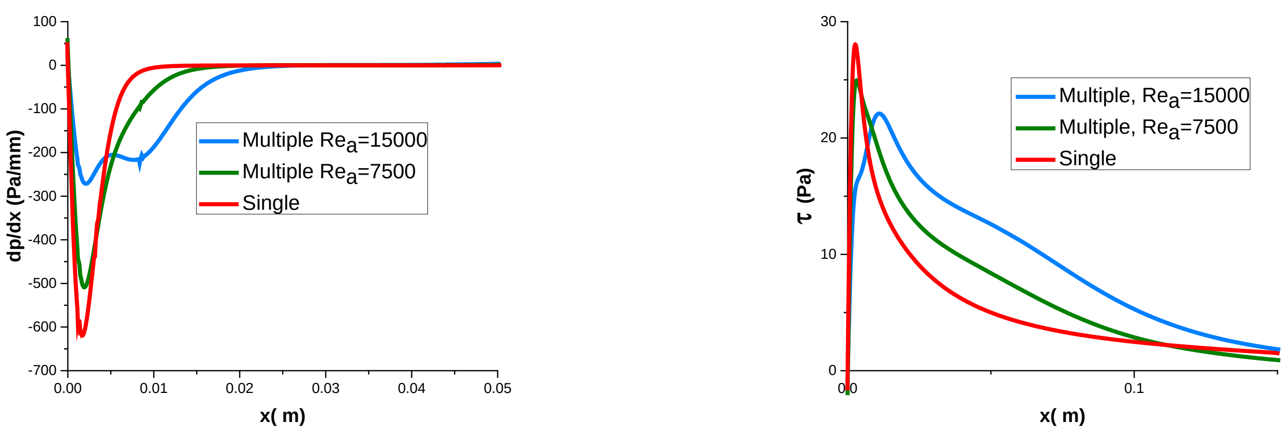

a b

Figure 8) Effect of auxiliary jet Reynolds number on a) wall pressure gradient and b) shear stress

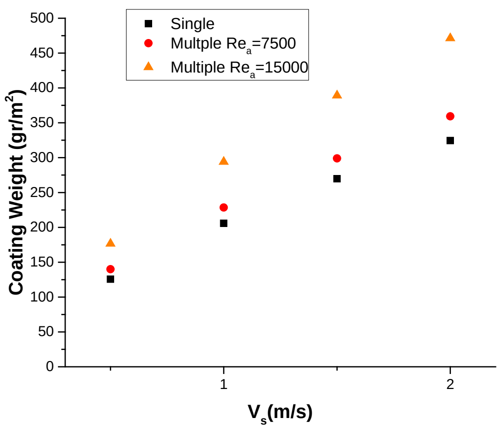

Figure 9) Effect of auxiliary jet Reynolds number on final coating weight

3.5. Effect of auxiliary jet offset

The effect of distance between the main and auxiliary jets exits "*s*" on shear stress and pressure gradient was investigated. Three different auxiliary jet offsets of *s*=20, *s*=10 and *s*=0 mm were considered and according to Figure 10 changing the auxiliary jet offset did not have a significant effect on final coating thickness because the maximum shear stress and maximum pressure gradient did not change significantly with changes in *s*. The comparison on Figure 10c shows that the final coating thickness would be thinner for the single jet wiping case.

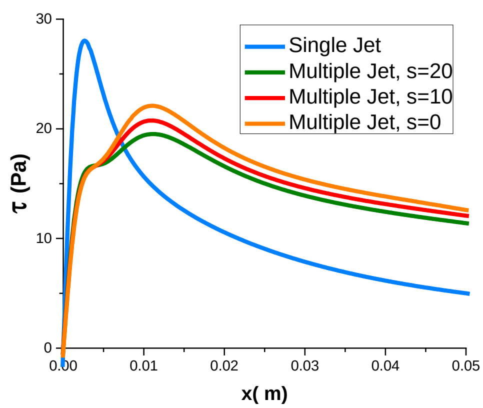

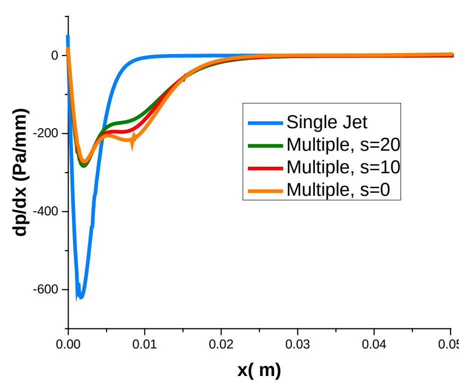

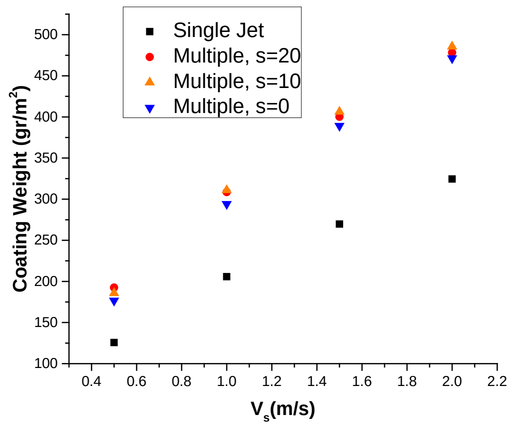

Figure 10) Effect of auxiliary jet offset "s" on wall shear stress, pressure gradient and final coating thickness where, Re_m=11000, Re_a=11000, z/d=6

4. Conclusion

Wall pressure and shear stress results from numerical simulations can be used as boundary conditions in the analytical solution of the liquid film thickness in order to estimate the final coating weight on a moving substrate. In the current study, the effects of jet to wall distance, auxiliary jet Reynolds number, strip velocity and auxiliary jet offset on coating thickness was investigated by numerical simulations of a multiple-slot impinging prototype design in comparison to the traditional single jet geometry. The pressure and shear stress results were validated using the experimental measurements of Ritcey [9]. It was observed that a thinner coating thickness can be achieved by decreasing the z/d ratio for both single and multiple slot cases. It was found that at a constant main jet Reynolds number, decreasing the auxiliary jet Reynolds number leads to decreasing coating weight. For a constant main and auxiliary jet Reynolds number, the location of the auxiliary jets has no significant effect on the final film thickness.

REFERENCES

1. J.A. Thornton, M.F. Graff, “An analytical description of the jet finishing process for hot-dip metallic coating on strip”, Metallurgical Transactions B 7B (1976), 607–618.

2. E.O. Tuck, “Continuous coating with gravity and jet stripping”, Physics of Fluids 26 (1983), 2352–2358.

3. C.H. Ellen, C.V. Tu, “An analysis of jet stripping of liquid coatings”, Journal of Fluids Engineering 106 (1984), 399–404.

4. K. Myrillasa, P. Rambauda, J.M. Mataigneb, P. Gardinb, S. Vincentc, J.M. Buchlina, “Numerical modeling of gas-jet wiping process” Chemical Engineering and Processing 68 (2013), 26– 31.

5. C.V. Tu, D.H. Wood, “Measurements beneath an impinging plane jet”, Experimental Thermal and Fluid Science 13 (1996), 364–373.

6. A. Gosset, J.M. Buchlin, P. Rambaud, M. Dubois, “Modeling of gas-jet wiping at small standoff distances”, 6th European Coating Symposium, Bradford, Great Britain, 2005.

7. J.M. Buchlin, “Modeling of gas-jet wiping, in: Thin Liquid Films and Coating Processes”, VKI Lecture Series, von Karman Institute for Fluid Dynamics, Belgium, 1997.

8. E.A. Elsaadawy, G.S. Hanumanth, A.K.S. Balthazaar, J.R. McDermid , A.N. Hrymak, J.F. Forbes, “Coating Weight Model for the Continuous Hot-Dip Galvanizing Process”, Metallurgical and Materials Transactions B 38 (2007), 413-424

9. A. Ritcey, J.R. McDermid, S. Ziada, F.E. Goodwin: “Parametric study of wall shear stress for coating weight models in continuous hot-dip galvanizing,” Galvatech 2015 Conf. Proceedings, Toronto, Canada, June 2015, pp. 690-696. 6.